Thermodynamically Irreversible Gating of Ryanodine Receptors in Situ Revealed by Stereotyped Duration of Release in Ca^{2+} Sparks

Shi-Qiang Wang,* Long-Sheng Song,* Le Xu,[†] Gerhard Meissner,[†] Edward G. Lakatta,* Eduardo Ríos,[‡] Michael D. Stern,* and Heping Cheng*

*Laboratory of Cardiovascular Sciences, National Institute on Aging, National Institutes of Health, Baltimore, Maryland 21224; [†]Department of Biochemistry and Biophysics, University of North Carolina, Chapel Hill, North Carolina 27599; and [‡]Department of Molecular Biophysics and Physiology, Rush University, Chicago, Illinois 60612 USA

ABSTRACT   For a single or a group of Markov channels gating reversibly, distributions of open and closed times should be the sum of positively weighted decaying exponentials. Violation of this microscopic reversibility has been demonstrated previously on a number of occasions at the single channel level, and has been attributed to possible channel coupling to external sources of free energy. Here we show that distribution of durations of Ca^{2+} release underlying Ca^{2+} sparks in intact cardiac myocytes exhibits a prominent mode at ~8 ms. Analysis of the cycle time for repetitive sparks at hyperactive sites revealed no intervals briefer than ~35 ms and a mode at ~90 ms. These results indicate that, regardless of whether Ca^{2+} sparks are single-channel or multi-channel in origin, they are generated by thermodynamically *irreversible* stochastic processes. In contrast, data from planar lipid bilayer experiments were consistent with *reversible* gating of RyR under asymmetric *cis* (4 μM) and *trans* Ca^{2+} (10 mM), suggesting that the irreversibility for Ca^{2+} spark genesis may reside at a supramolecular level. Modeling suggests that Ca^{2+}-induced Ca^{2+} release among adjacent RyRs may couple the external energy derived from Ca^{2+} gradients across the SR to RyR gating in situ, and drive the irreversible generation of Ca^{2+} sparks.

INTRODUCTION

The ryanodine receptor (RyR), an intracellular Ca^{2+} release channel (Meissner, 1994), is widely distributed in many types of cells and plays an essential role in diverse physiological processes, including synaptic plasticity (Hong et al., 2000), muscle contraction (Franzini-Armstrong and Protasi, 1997; Bers, 2000), and cell survival and death (Marks, 1997). In striated muscles it constitutes an essential component of excitation-Ca^{2+} release (EC) coupling, whereby a depolarization across the transverse tubule (TT) membrane leads to rapid release of Ca^{2+} from the sarcoplasmic reticulum (SR). The RyR has been extensively characterized as a Ca^{2+} and monovalent cation channel in planar lipid bilayers and other subcellular experimental systems. Like the vast majority of ionic channels, single RyRs in vitro have been described by Markovian models (Ashley and Williams, 1990; Tinker et al., 1992; Cheng et al., 1995; Zahradnikova and Zahradnik, 1996; Zahradnikova et al., 1999), in which transition between discrete conformational states is determined solely by the present state of the channel, independent of history (only beyond 10–20 transitions; see Ashley and Williams, 1990). When such a channel is unperturbed, i.e., uncoupled from an external source of energy, thermodynamic laws require microscopic reversibility of the channel reaction. This means that, at equilibrium, a

cyclic reaction must take place at the same rate in forward and backward directions, the stochastic properties of the channel must show time reversibility, and distributions of statistical quantities, such as open time, closed time, and burst time, must each equal a sum of positively weighted, decaying exponential terms (Colquhoun and Hawkes, 1995). The same conclusions are applicable for a cluster of interlinked channels that are uncoupled to an external energy source, because such cluster as a whole can be treated as a Markovian entity.

Although extremely rare, a number of ion channels have been shown to violate the microscopic reversibility at the single channel level. For instance, a modal open time distribution was observed for glutamate receptors/channels (Gration et al., 1982), and asymmetric (i.e., time-irreversible) transitions between subconducting states were found for a mutant NMDA channel (Schneggenburger and Ascher, 1997). Molecular mechanisms underlying the irreversible behavior in these cases were generally unclear, although it was proposed that channel gating must somehow couple to the electrochemical gradients of the permeating ions. Asymmetric currents were also reported for a Torpedo Cl$^-$ channel (Richard and Miller, 1990), and were recently attributed to the role of Cl$^-$ ions in modulating voltage-dependent gating of the channel (Chen and Miller, 1996). The dual role of Ca^{2+} as both a permeating ion and a regulator of RyR channel (Tripathy and Meissner, 1996; Xu and Meissner, 1998) creates the intriguing possibility that RyR gating might be coupled to the free energy in Ca^{2+} electrochemical gradients across the SR. If this were the case, RyRs in intact cells (or in bilayers under asymmetric Ca^{2+} electrochemical potentials) might be expected to gate irreversibly.

Because of their intracellular location, RyRs in intact cells have thus far defied direct electrophysiological measurement. However, the discovery of Ca^{2+} sparks in excitable (Cheng et al., 1993; Nelson et al., 1995; Tsugorka et al., 1995; Klein et al., 1996) and nonexcitable (Haak et al., 2001) cells has provided an alternative means by which RyR activity in situ can be observed noninvasively. Although initial evidence was ambivalent (Cheng et al., 1993), the view now prevalent is that more than one RyR from a release unit, or "couplon" (Stern et al., 1999), contribute to a spark (Bridge et al., 1999; González et al., 2000a; Izu et al., 2001; Wang et al., 2001). Investigation of the properties of Ca^{2+} sparks may provide insightful information regarding the nature of RyR gating in the physiological environments of intact cells. In the present study we sought and have identified fingerprints of irreversible gating of RyRs in situ, and explored the possible physiological significance of irreversibility in shaping the elemental Ca^{2+} signaling events.

METHODS

Cell preparation

Ventricular cardiac myocytes were isolated from adult Sprague-Dawley rats (2–3 months old, weight 225–300 g) using standard enzymatic techniques, as described previously (Zhou et al., 2000). Freshly isolated single cells were stored in Tyrode's solution containing (in mM) 137 NaCl, 5.4 KCl, 1.2 MgCl₂, 1 NaH₂PO₄, 1 CaCl₂, 20 glucose, and 20 HEPES (pH 7.4). All experiments were performed at room temperature (20–22°C).

Visualization of spontaneous Ca²⁺ spikes and Ca²⁺ sparks

Myocytes were whole-cell voltage-clamped at −60 mV with patch pipettes (1.5–2.5 MΩ) and superfused with Tyrode's solution. Ca^{2+} release fluxes in the resting cell were detected with the low-affinity Ca^{2+}-sensitive dye Oregon Green 488 BAPTA-5N (OG-5N, Molecular Probes, Eugene, OR) (1 mM) in conjunction with 4 mM [EGTA], as described previously (Song et al., 1998). Confocal images were acquired using a Zeiss LSM-410 inverted confocal microscope with a Zeiss Plan-Neofluor 40× oil immersion objective (NA = 1.3), and confocal pinhole set to render spatial resolutions of 0.4 μm in the x-y axis and 0.9 μm in the z-axis. OG-5N was excited by an argon laser (488 nm), and fluorescence was measured at >515 nm. Images were taken in the line-scan mode, with the scan line parallel to the long axis of the myocytes. Each image consisted of 512 line scans obtained at 2.09-ms intervals, each comprising 512 pixels at 0.10 μm separation. The pipette solution contained (in mM) 105 CsCl, 10 NaCl, 5 MgATP, 10 HEPES, 20 TEA-Cl, 4 EGTA, 2 CaCl₂, and 1 OG-5N (pH 7.2). In some experiments spontaneous Ca^{2+} sparks were observed under the same experimental conditions, except that EGTA and OG-5N in the pipette filling solution were replaced by 0.15 mM Fluo-3.

Single channel measurements

Single channel measurements were performed by fusing proteoliposomes containing the purified RyR2 with Mueller-Rudin-type bilayers containing phosphatidylethanolamine, phosphatidylserine, and phosphatidylcholine in the ratio 5:3:2 (25 mg of total phospholipid per ml n-decane) (Lee et al., 1994). The side of the bilayer to which the proteoliposomes were added

was defined as the *cis* side. A strong dependence of channel activity on [Ca^{2+}] in the *cis* side showed that it corresponded to the SR cytosolic side. The *trans* side of the bilayer was defined as ground. Single channels were recorded at 0 mV in symmetric KCl buffer solution (0.25 M KCl, 20 mM KHEPES, pH 7.4) containing 10 μM *cis* and 10 mM *trans* Ca^{2+}. Electrical signals were filtered at 300 Hz, digitized at 10 kHz, and analyzed. Data acquisition and analysis were performed with a commercially available software package (pClamp 6.0.3, Axon Instruments, Burlingame, CA).

Calibration of EGTA/OG-5N response to Ca²⁺ pulse

The calibration solution contained (in mM) 140 KCl, 10 NaCl, 10 HEPES, 0.2 NP-EGTA, 1 OG-5N, 0–4 EGTA. CaCl₂ was added accordingly to yield a free Ca^{2+} concentration of 150 nM. PH was adjusted to 7.2. Transient increases of [Ca^{2+}] were produced by photolysing NP-EGTA-Ca, using 6-ns UV laser pulses (Quanta-Ray INDI pulsed Nd:YAG laser, Spectral Physics Lasers, Inc., Mountain View, CA). The OG-5N fluorescence was sampled by confocal microscopy at 29.2 μs time resolution.

Data analysis

All confocal images of indicator fluorescence (F) were normalized to basal fluorescence (F_0) and expressed as F/F_0. Image data were processed by using IDL software (Research System, Boulder, CO) and a modified spark detection algorithm (Cheng et al., 1999). All quantitative data were expressed as mean ± SEM.

RESULTS

Duration of Ca²⁺ sparks measured in the presence of 4 mM EGTA

To directly measure RyR active time underlying Ca^{2+} sparks, cardiac myocytes were dialyzed, via the patch pipette, with 4 mM EGTA, a high-affinity and slow Ca^{2+} buffer, and 1 mM OG-5N, a fast and low-affinity Ca^{2+} indicator. The (binding reaction to the) fast indicator follows the local [Ca^{2+}] near release sites much more closely than the buffer. Because the local [Ca^{2+}] under highly buffered conditions is proportional to release flux (Ríos and Pizarro, 1991; Pape et al., 1995; Song et al., 1998), the fluorescence signal from OG-5N therefore tracks the Ca^{2+} release flux (Song et al., 1998).

Fig. 1 *A* shows in a representative cell under steady-state conditions (holding potential = −60 mV), that spontaneous discharging of Ca^{2+} into the cytosol can be visualized as infrequent, discrete "Ca^{2+} spikes" by confocal line-scan imaging. These spikes were localized to the TT/Z-line region of a sarcomere, and were completely abolished by ryanodine (5 μM, 3 min; data not shown), indicating correspondence with Ca^{2+} sparks (Cheng et al., 1993). Ca^{2+} spikes were highly confined in space, with a full-width at half-maximum (FWHM) of 0.65 ± 0.02 μm (n = 130), which is comparable to dimensions of the point spread function of the confocal imaging system (FWHM = 0.4 and 0.9 μm in the lateral and axial directions, respectively). This observation suggests that a Ca^{2+} spark normally arises from

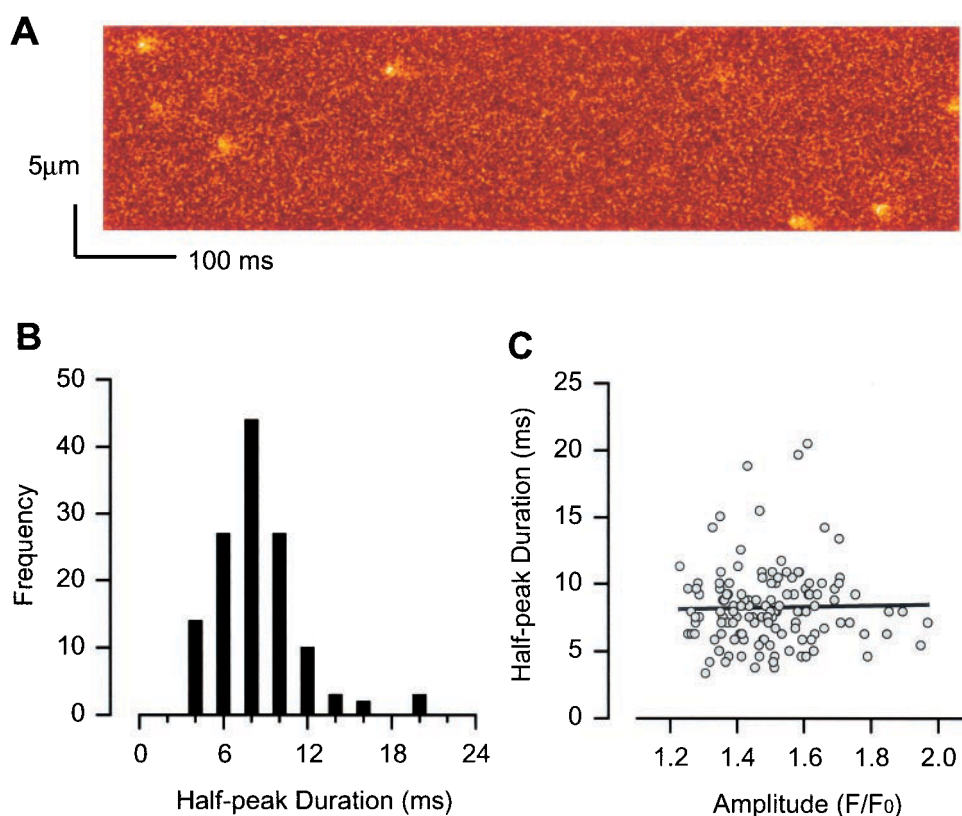**A**

5µm

100 ms

B

C

FIGURE 1 Duration of spontaneous Ca^{2+} spikes recorded with the fast Ca^{2+} indicator OG-5N (1 mM) combined with EGTA (4 mM) in cardiac myocytes. (*A*) A confocal image of representative Ca^{2+} spikes at a holding potential of -60 mV. The time courses of Ca^{2+} spikes (traces beneath the image) provide a measure of Ca^{2+} release function during Ca^{2+} sparks. (*B*) Histogram distributions for spike half-peak duration. Note that Ca^{2+} release duration for the randomly sampled population of Ca^{2+} spikes exhibits a prominent mode, in contrast to what is predicted from reversible channel gating. (*C*) Scatter plot of spike duration as a function of spike amplitude. Linear regression of the data (straight line) reveals no significant correlation between amplitude and duration of Ca^{2+} spikes.

a rather small, or even a "point," source of Ca^{2+} within a single TT-SR junction (see Parker and Wier, 1997, and Blatter et al., 1997, for exceptions).

In contrast to conventional Ca^{2+} sparks, which last $\sim$20–30 ms, Ca^{2+} spikes, or Ca^{2+} release functions of the sparks, were very brief (Fig. 1 *A*). We next quantified the half-peak duration of Ca^{2+} spikes to estimate active duration of the release unit. The histogram distribution of spike duration is shown in Fig. 1 *B*. Durations were rather stereotyped, with a mode at 8 ms and a standard deviation (σ) of 2.8 ms. Spike durations, therefore, do not have a monotonically declining exponential distribution, in contrast to what would be expected for a microscopically reversible gating mechanism.

Several potential artifacts require consideration. First, because Ca^{2+} spikes detected by confocal microscopy consist of both in-focus and out-of-focus events, sampling presents a major problem confounding measurement of spark amplitude (Pratusevich and Balke, 1996; Smith et al., 1998; Cheng et al., 1999; Ríos et al., 2001), and thus might obscure the true duration distribution. Fortunately, because EGTA restricts Ca^{2+} diffusion from the release site, the

out-of-focus detection appeared to have little impact on the measurement of spike kinetics. As shown by the scatter plot and regression analysis in Fig. 1 *C*, there was no significant correlation between spike amplitude and duration. In other words, the dim spikes, which tend to be farther away from the scan line, exhibit similar durations as the bright spikes, which tend to be closer to the scan line. This indicates that confocal microscopy can faithfully track the ignition and termination of Ca^{2+} spikes, regardless of their locations, and is consistent with simulations indicating that spark's rise time, corresponding to the duration of the underlying release, is perhaps the most robust spark parameter against sampling errors (Smith et al., 1998).

Second, the preferred spike duration might also be attributable to a finite response time of the OG-5N/EGTA system to Ca^{2+} flux, which broadens apparent spike duration and might render an artificial mode in duration distribution. To test this possibility, we calibrated the response kinetics of OG-5N in solutions containing various concentrations of EGTA. In response to a sudden increase in Ca^{2+} elicited by liberating NP-EGTA caged Ca^{2+} with a 6-ns laser flash, the OG-5N signal peaked in $\sim$100 μs, irrespective of EGTA
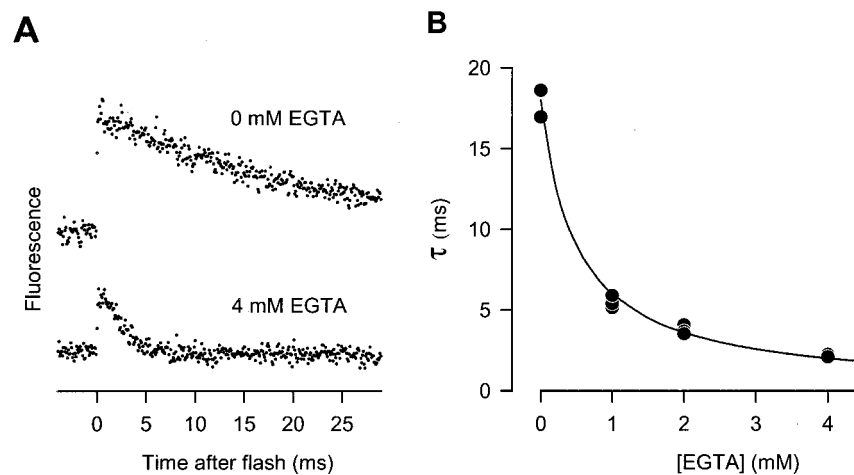
FIGURE 2 Kinetic calibration of the OG-5N/EGTA system. (*A*) Representative OG-5N fluorescence traces obtained with 0 and 4 mM EGTA. Note that the peak, the decaying kinetics, and the steady-state OG-5N signal after flash depend on [EGTA] used. Calibration solution was composed of (in mM) 140 KCl, 10 NaCl, 10 HEPES, 0.2 NP-EGTA, 0.15 CaCl₂, 1 OG-5N, and 0–4 EGTA. A Ca²⁺ pulse was elicited by uncaging Ca²⁺ from NP-EGTA-Ca²⁺ with a single 6-ns UV laser flash. (*B*) Relationship between the decay time constant (τ) and [EGTA]. Data were fitted to a hyperbolic function, $\tau = 8.99/([EGTA] + 0.505)$ (*solid line*).

concentration. However, the decay of the signal was markedly accelerated in the presence of 1–4 EGTA (Fig. 2 *A*). The relationship between the decay time constant (τ) of OG-5N fluorescence and EGTA concentration ([EGTA]) was fit by the hyperbolic function $\tau = 8.99/([EGTA] + 0.505)$ (Fig. 2 *B*).

In 4 mM EGTA, the half-decay time was 1.5 ms. Hence, the lag and hysteresis of the OG-5N/EGTA response appear to be too brief to account for the appearance of the mode at 8 ms in spike duration. Thus, the mode in the duration histogram of Ca²⁺ spikes provides evidence that RyRs gate irreversibly during a Ca²⁺ spark.

Ca²⁺ spark amplitude, rise time, and cycle length for events from the same location

Albeit infrequently, spontaneous Ca²⁺ sparks can occur repetitively at the same locations in cardiac (Cheng et al., 1993; Parker and Wier, 1997) or skeletal (Klein et al., 1999) myocytes. Characterization of such repetitive sparks should be instructive because it eliminates the variance introduced by out-of-focus detection. Fig. 3 *A* illustrates a representative sequence of repetitive Ca²⁺ sparks in a rat cardiac myocyte at −60 mV holding potential. A total of 104 events from the hyperactive site were registered in 11 consecutive images taken over a period of 9 min. The statistics did not differ significantly between images, or between the first and the second halves of the data, suggesting that spark generation was stationary during the period of observation. Fig. 3 *B* shows that the spark amplitude is narrowly distributed around $F/F_0 = 2.62$, with a $\sigma = 0.23$ (the baseline fluorescence $\sigma = 0.14$) (Fig. 3 *B*). It is also noteworthy

that there is little correlation between the spark amplitude and the corresponding cycle time, suggesting variation in spark amplitude is not related to local SR Ca²⁺ filling status in this case. This observation is in agreement with previous reports (Bridge et al., 1999), and can be explained by either irreversible channel gating (Shirokova et al., 1999; Ríos et al., 2001) or collective behavior of a group of channels (Bridge et al., 1999). Furthermore, the bright and sharp appearance of these sparks suggests they were near- or in-focus events (Ríos et al., 2001).

Numerical analysis indicates that a spark decays immediately after cessation of the release flux (e.g., Smith et al., 1998), and thus the rise time of Ca²⁺ sparks provides a good estimate of the underlying Ca²⁺ release duration. Indeed, the mean rise time of these repeats (7.37 ms) was highly comparable with half-peak duration of Ca²⁺ spikes in Fig. 1 (8.25 ms). Similar to spike duration, the spark rise time duration featured a central mode at 7 ms with $\sigma = 1.7$ ms (Fig. 3 *C*). Therefore, the distribution patterns for spark rise time and for Ca²⁺ spike duration both indicate a preferred active duration of RyRs during a spark, and are thus incompatible with reversible gating of RyRs in Ca²⁺ spark genesis.

If RyRs gate reversibly, the cycle time for these repeats should also feature a monotonic decreasing distribution. However, Fig. 3 *D* shows that this is not the case: the shortest interval between two consecutive sparks was 38 ms, evincing an absolute refractory period after the occurrence of a spark. The events in the 40-ms bin were considerably fewer than those in the 60-, 80-, or 100-ms bins, suggesting a relative refractory period, and giving rise to a mode at ~90 ms. The existence of a mode in cycle time distribution further substantiates the idea that
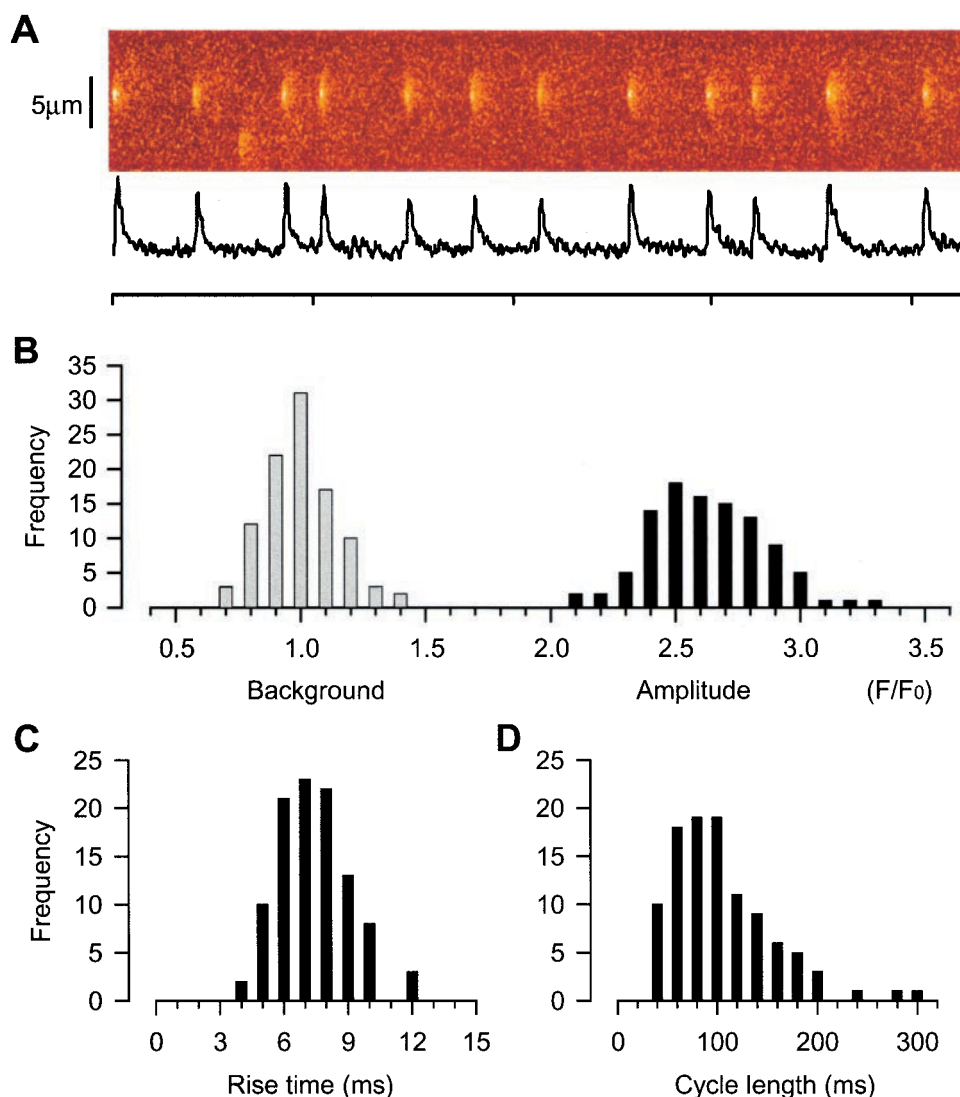
FIGURE 3 Amplitude, rise time, and cycle length of spontaneous Ca^{2+} sparks at a fixed site. (A) A typical confocal line scan image record. A total of 104 events from the hyperactive site were registered in 11 consecutive images taken over a period of 9 min in a rat cardiac myocyte at a holding potential of −60 mV. (B) Histogram distributions of spark amplitude (*solid bars*) and randomly sampled baseline (*open bars*). (C and D) Histograms for spark rise time (C) and cycle length (D).

spark genesis is driven by thermodynamically irreversible Markovian processes.

Open and closed time distribution of single RyRs in planar lipid bilayers

One possible mechanism that drives the irreversible gating of RyRs in intact cardiac myocytes might be a coupling of the free energy in Ca^{2+} gradients to channel gating. In this respect, Ca^{2+} in the cytosol is known as the physiological activator of RyRs, and multiple putative regulatory Ca^{2+} binding sites have been identified on the channel protein. We therefore measured single cardiac RyR activity incorporated in a planar lipid bilayer in the presence of asym-

metric Ca^{2+} (4 μM *cis* and 10 mM *trans*) at a voltage of 0 mV (Fig. 4 *A*). Under these experimental conditions the open time histogram, plotted in Fig. 4 *B* on a semi-log scale, was well-fitted by three positively weighted exponential functions, with time constants $\tau_1 = 1.0$, $\tau_2 = 6.2$, and $\tau_3 = 92.7$ ms. Similarly, the closed time histogram was also fitted by three positive exponentials, with decaying time constants $\tau_1 = 1.7$, $\tau_2 = 14.2$, and $\tau_3 = 66.5$ ms (Fig. 4 *C*). Qualitatively similar results were obtained for skeletal RyRs at the single channel level with 10 μM *cis* and 10 mM *trans* Ca^{2+} (data not shown). Hence, single cardiac and skeletal RyRs gating in vitro do not show any "anomalous" mode in open and closed time distributions in the presence of a steep transmembrane Ca^{2+} gradient ($\geq 10^3$ folds).
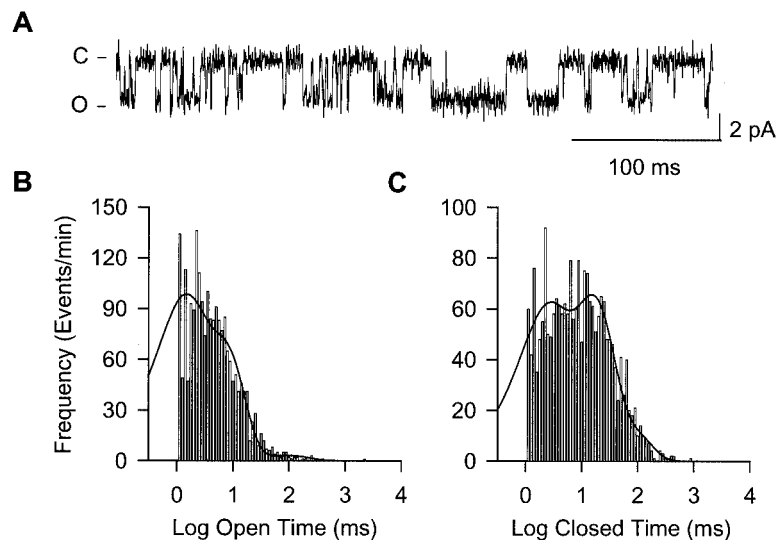
FIGURE 4   Single channel current and maximum likelihood fits of time histograms. (*A*) A single cardiac RyR ion channel was incorporated in a lipid bilayer. Single channel currents were recorded at 0 mV (downward deflection from closed level (c–) in symmetric 0.25 M KCl, pH 7.4 solutions containing 10 mM lumenal Ca^{2+} and 4 μM cytosolic Ca^{2+}. (*B* and *C*) Open (*B*) and closed (*C*) time histograms were well-fitted by three (open time) or three (closed time) exponential functions (*solid lines*) with (*B*) $a_1 = 0.476$, $a_2 = 0.502$, $a_3 = 0.022$, $\tau_1 = 1.0$, $\tau_2 = 6.2$, $\tau_3 = 92.7$ ms; and (*C*) $a_1 = 0.359$, $a_2 = 0.529$, $a_3 = 0.113$, $\tau_1 = 1.7$, $\tau_2 = 14.2$, and $\tau_3 = 66.5$ ms (*C*), respectively.

Numerical analysis of Ca^{2+}-driven irreversible gating of single or clustered RyRs

Several possibilities could account for the qualitative discrepancy regarding the reversibility of RyR gating in vivo and in vitro (see Discussion). A plausible reason is that, due to restricted electrodiffusion of Ca^{2+} ions in the junctional cleft (Soeller and Cannell, 1997), RyR may sense a lower local [Ca^{2+}] in vitro and thus manifest little irreversible effect. To explore this possibility we resorted to computer modeling and numerical simulations. Fig. 5 illustrates a possible role of local [Ca^{2+}] as a timing mechanism of open duration of a contrived RyR channel. Once the channel is open the local [Ca^{2+}] surpasses the ambient [Ca^{2+}] (set at 100 nM). The increased local [Ca^{2+}] promotes clockwise transition between different open states (Fig. 5, *A* and *B*); the passage through the consecutive states has a preferred time and thus creates an "anomalous" mode in the open time distribution. It is clear that the mode becomes more prominent at higher local [Ca^{2+}] (Fig. 5, *B* and *C*), indicating Ca^{2+} gradients as the time-keeping mechanism of the "clock" model of RyR, but disappears when [Ca^{2+}] = 0.1 μM, i.e., [Ca]$_{local}$ = Ca$_0$ (Fig. 5 *B*), in conformity with thermodynamic laws.

Alternatively, the irreversible RyR gating during spark genesis may reflect the collective behavior of a group of RyRs in a "couplon" (i.e., a diad junction). We used the stochastic local-control model of cardiac EC coupling (Stern et al., 1999) to generate histograms of couplon active duration. In this model the RyR gating scheme has only one open state, and individual RyRs are Markovian channels

with the opening duration distributed monoexponentially (Fig. 6 *A*). However, strong irreversible interactions among RyRs are mediated by released Ca^{2+} in the junctional cleft. If the open event is, instead, considered to be the activation of a couplon, the distribution has a clear modal component (Fig. 6 *B*), due to the local recruitment of RyRs driven by permeating Ca^{2+} via the Ca^{2+}-induced Ca^{2+} release (CICR) mechanism (Endo et al., 1970; Fabiato, 1985). If permeation is abolished, by setting SR luminal [Ca^{2+}] to zero, the couplon activation histogram exhibits monotonic decay because in this case the entire array of RyRs becomes a single, reversible Markovian chain.

DISCUSSION

Ca^{2+} spark genesis as an irreversible Markov process

Whether RyR gating underlying Ca^{2+} sparks is a thermodynamically reversible Markovian process is of fundamental interest, both with respect to the nature of Ca^{2+} sparks and RyR physiology. Much previous work has focused on spark amplitude as the readout of how RyRs behave within the cell. Theory (Cheng et al., 1999; Ríos et al., 2001) and numerical analysis (Pratusevich and Balke, 1996; Smith et al., 1998) have shown that *apparent* Ca^{2+} spark amplitudes recorded by confocal microscopy should always display a monotonic decaying distribution, regardless of their *true* amplitude distribution. Experimental measurements with the aid of an automated detection algorithm (Cheng et al., 1999) have confirmed it. In an attempt to reveal true spark
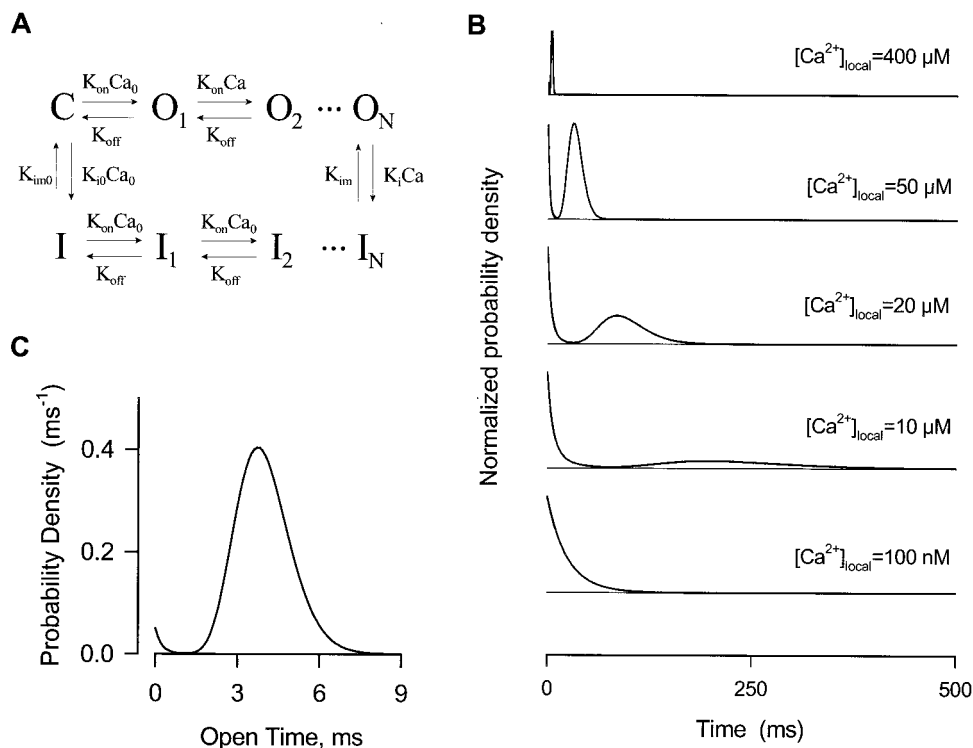
FIGURE 5 $[Ca^{2+}]$ as a timing mechanism of RyR open time duration. (*A*) A contrived RyR model, where $K_{on} = 10$ ms^{-1} mM^{-1}; $K_{off} = 0.04$ ms^{-1}; $K_i = 12.8$ ms^{-1} mM^{-1}; $K_{im} = 0.000078125$ ms^{-1}; $K_{im0} = K_{im}$; Ca$_0 = 0.0001$ mM (ambient $[Ca^{2+}]$ with the channel closed); Ca = local $[Ca^{2+}]$ when the channel is open; and K_{io} is determined by microscopic reversibility under equilibrium conditions (Ca = Ca$_0$). (*B*) Channel open duration at various local $[Ca^{2+}]$ ranging from 100 nM to 400 μM. Note that the shape of distribution curve is no longer monotonically decreasing at local $[Ca^{2+}]$ higher than 100 nM, violating the microscopic reversibility. Note also that the increase in local $[Ca^{2+}]$ initially prolongs, but then abbreviates, the channel mean open time. This reproduces a recent experimental finding on a biphasic dependence of RyR open duration on local $[Ca^{2+}]$ (Xu and Meissner, 1998). Interestingly, the abbreviation of channel open time at high local $[Ca^{2+}]$ is due not only to a Ca^{2+}-dependent inactivation (O$_N$-I$_N$ in *A*), but more importantly, to a Ca^{2+}-driven rapid passage through the open states (O$_1$-O$_2$-$\cdots$-O$_N$). (*C*) Open time distribution at 400 μM local $[Ca^{2+}]$ on an expanded time scale. Because the local $[Ca^{2+}]$ is much greater than the ambient $[Ca^{2+}]$, the clockwise reaction predominates the counterclockwise reaction, and the local high $[Ca^{2+}]$ propels the channel through multiple consecutive open states, giving rise to a preferred open duration.

amplitudes, Bridge et al. (1999) tracked Ca^{2+} sparks evoked at fixed positions during excitation-contraction coupling (with the L-type Ca^{2+} channels largely blocked) and demonstrated a rather stereotyped amplitude distribution. Similar results were obtained in the present study for spontaneous Ca^{2+} sparks from a hyperactive site (Fig. 3). Application of a mathematical deconvolution algorithm (Izu et al., 1998; González et al., 2000a) also unmasked a non-monotonic distribution of amplitudes for randomly sampled, depolarization-evoked Ca^{2+} sparks in a subset of skeletal muscle fibers (Ríos et al., 2001). Caffeine at low doses, which sensitizes CICR without depleting the SR, reversibly induces or enhances the mode in the amplitude distribution (Ríos et al., 2001). Most recently, we have performed the first direct measurement of in-focus Ca^{2+} sparks evoked beneath the patch membrane in intact cardiac myocytes, and our results confirmed a broad modal amplitude distribution (Wang et al., 2001). The modality of the spark amplitude distribution was initially interpreted to reflect a multi-RyR origin of sparks (Bridge et al., 1999).

Alternatively, it could be a manifestation of irreversible gating of a single RyR (Shirokova et al., 1999; Ríos et al., 2001). If Ca^{2+} sparks have a multi-channel origin, however, a modal amplitude does not rule out reversibility in the underlying process.

A hallmark of irreversible single-channel gating is the anomalous "mode" in the distribution of open or closed times. For a group of Markovian channels the active time (presence of one or more channels opening, akin to subconducting states of a single channel) can be similarly exploited to detect irreversibility of the channel group. In a recent study we used spark rise time to estimate the Ca^{2+} release duration and demonstrated the presence of a mode in the distribution of spark rise time (González et al., 2000b) or in the joint distribution of rise time and spatial width for evoked Ca^{2+} sparks in skeletal muscle (Ríos et al., 2001). Caffeine shifts the mode upward, from ~4 ms to ~8 ms, or creates a de novo mode in the joint distribution of rise time and spatial width. In the present study we used Ca^{2+} spikes as a direct measurement of the Ca^{2+} release function of
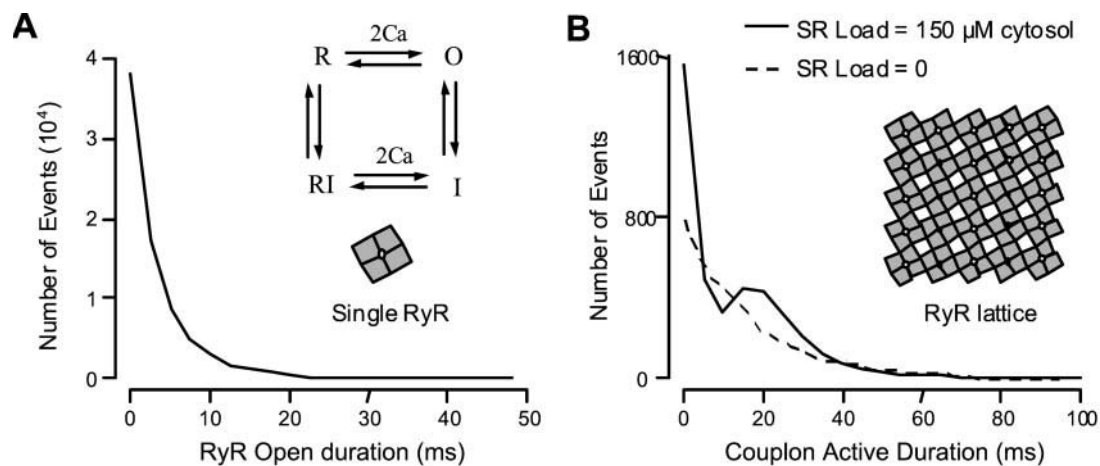
FIGURE 6 A couplon model: local CICR as a timing mechanism. A stochastic local-control model of cardiac excitation-contraction coupling was generated as in Stern et al. (1999). (*A*) RyR gating scheme used (*inset*) and the corresponding open time distribution. (*B*) Distribution of duration of couplon activation (presence of one or more open RyRs in a diad junctional complex containing a 5 × 5 array of RyRs). The *inset* shows disposition of RyRs in the release unit. Their gating scheme is the same as in *A*. See Stern et al. (1999) for intra-couplon Ca^{2+} gradients that drive irreversible gating of the unit. The distribution has a clear modal component due to the local recruitment of RyRs by CICR driven by permeating Ca^{2+}. As expected, the mode disappears when the SR luminal [Ca^{2+}] is set to zero.

Ca^{2+} sparks. Calibration in homogenous solution showed that the OG-5N/EGTA system response follows the flux with an ~1.5 ms lag. For detection of Ca^{2+} spikes where Ca^{2+} emanates from a point source, the "off" kinetics should be further sharpened because of outward diffusion of local Ca^{2+} and inward diffusion of fresh Ca^{2+} buffers. Moreover, the limited spatial expansion of Ca^{2+} spikes ensures that confocal detection does not distort Ca^{2+} spike kinetics. Under these conditions we found that spontaneous cardiac Ca^{2+} sparks have a stereotypical release duration with a central mode at 8 ms (Fig. 1). Furthermore, by analyzing spark rise time at a fixed release site undergoing a stationary hyperactivity, we found a similar modal distribution of release duration in the absence of EGTA (Fig. 3). A more striking deviation from a monotonic distribution was identified for the cycle time, as shown by the lack of intervals below 38 ms and the presence of a mode at ~90 ms (Fig. 3). Thus, the present study affords several lines of evidence that Ca^{2+} sparks are generated by irreversible Markovian processes in cardiac myocytes. Additional evidence of irreversible RyR gating in situ has been obtained based on oscillating macroscopic release waveforms in skeletal muscle (Rengifo et al., 2001).

Although the above conclusion is in general agreement with our recent findings in skeletal muscle (Ríos et al., 2001), there is an important distinction between spontaneous versus evoked events with respect to thermodynamic analysis. In contrast to evoked sparks, the spontaneous events are uncoupled from either L-type channel Ca^{2+} influx or the voltage sensor in the plasma membrane (as in skeletal muscle), and emerge from a system under steady-state conditions. The appraisal of irreversibility for such a

stationary Markovian process is greatly simplified relative to that for non-steady-state phenomena.

Possible source of energy driving irreversible RyR gating in situ

Since spontaneous Ca^{2+} sparks are uncoupled from the plasma membrane, a possible source of energy driving the irreversible RyR gating must be inherent to the SR Ca^{2+} release unit and its associated regulatory system. Previous in vitro experiments have raised the possibility of coupling between permeating ions and channel gating as the mechanism of irreversibility (Tripathy and Meissner, 1996; Xu and Meissner, 1998). In this regard coupling of the SR Ca^{2+} gradients to RyR gating not only is feasible, but also could be powerful, as the SR membrane separates Ca^{2+} concentrations at a ratio of 10^3-10^4 (Bers, 2000). The question then is whether the coupling, and thereby the irreversibility, occur at the single channel or the release unit or couplon level. The planar lipid bilayer data presently available suggest that single RyRs in vitro behave as reversible Markov processes, even in the presence of steep Ca^{2+} gradients (Fig. 4) (Tinker et al., 1992; Xu and Meissner, 1998; Zahradnikova et al., 1999). It is thus less likely, albeit not impossible (Fig. 5, and see below), that individual RyRs gate irreversibly in vivo.

At the supramolecular level two mechanisms have been proposed for inter-RyR communication: CICR (Endo et al., 1970; Fabiato, 1985) and FK506 binding protein (FKBP)-coupled gating of RyRs (Marx et al., 1998). In planar lipid bilayers, FKBP, a RyR accessory protein, can link individual RyRs to gate synchronously, as if they were a single

channel of multiplied conductance (Marx et al., 1998). This particular mechanism has been invoked to explain the sharp onset and offset of Ca^{2+} sparks (Stern et al., 1999): allosteric interaction may reciprocally shunt free energy from one RyR to the nearest neighbors in physical contact, in a state-dependent manner, making asynchronous transitions of RyRs unfavorable thermodynamically. However, in this hypothesis microscopic reversibility would still apply to the collective release unit, which excludes coupled gating as candidate mechanism for irreversible spark generation.

If, as discussed above, RyRs appear to be uncoupled from the permeating Ca^{2+} at the single channel level, could CICR still provide the free energy to drive irreversible spark genesis? The answer is affirmative, as demonstrated in Fig. 6. In this model, the irreversibility is a collective behavior manifested only for a group of RyRs, and in the presence of Ca^{2+} gradient across the SR. Mechanistically, while the free energy in Ca^{2+} gradients tapped by an open RyR cannot retrogradely affect its own gating (Fig. 6 A), it can still propel irreversibility at the release unit or couplon level if it is effectively coupled to the gating of its neighboring RyRs (Fig. 6 B). This result sheds a new light on the logic that underlies clustering of RyRs in many types of cells.

It is generally accepted that increasing the SR Ca^{2+} content beyond a critical level greatly enhances RyR sensitivity to bolster unstable CICR (e.g., Diaz et al., 1996). The converse effect, i.e., whether decreasing RyR Ca^{2+} negatively regulates RyR gating and thereby terminates the SR Ca^{2+} release remains controversial (Song et al., 1997; Bers, 2000). In any case, a role of partial local depletion of SR Ca^{2+} played in the shut-off of RyRs during a spark could provide another coupling between RyR gating and the SR Ca^{2+} gradients. Finally, gating of RyRs in intact cells could be more complex than what is gleaned above if RyR gating coupled to chemical reactions to harness external free energy. For instance, RyRs in cells are tightly associated with protein kinases (protein kinase A) and phosphatases (PP1 and PP2a) in the RyR signaling complex (Marx et al., 2000), and thus may undergo rapid phosphorylation and dephosphorylation, in a Ca^{2+}- or conformational state-dependent fashion, which then prohibits or catalyzes transitions between certain RyR states. Critical examination of the involvement of local Ca^{2+} and other regulatory mechanisms in the genesis of Ca^{2+} sparks leading to irreversible RyR gating is called for in future studies.

REFERENCES

Ashley, R. H., and A. J. Williams. 1990. Divalent cation activation and inhibition of single calcium release channels from sheep cardiac sarcoplasmic reticulum. *J. Gen. Physiol.* 95:981–1005.

Bers, D. M. 2000. Calcium fluxes involved in control of cardiac myocyte contraction. *Circ. Res.* 87:275–281.

Blatter, L. A., J. Hüser, and E. Ríos. 1997. Sarcoplasmic reticulum Ca^{2+} release flux underlying Ca^{2+} sparks in cardiac muscle. *Proc. Natl. Acad. Sci. U.S.A.* 94:4176–4181.

Bridge, J. H., P. R. Ershler, and M. B. Cannell. 1999. Properties of Ca^{2+} sparks evoked by action potentials in mouse ventricular myocytes. *J. Physiol.* 518:469–478.

Chen, T., and C. Miller. 1996. Nonequilibrium gating and voltage dependence of the ClC-0 Cl channel. *J. Gen. Physiol.* 108:237–250.

Cheng, H., M. Fill, H. Valdivia, and W. J. Lederer. 1995. Models of Ca^{2+} release channel adaptation. *Science.* 267:2009–2010.

Cheng, H., W. J. Lederer, and M. B. Cannell. 1993. Calcium sparks: elementary events underlying excitation-contraction coupling in heart muscle. *Science.* 262:740–744.

Cheng, H., L. S. Song, N. Shirokova, A. González, E. G. Lakatta, E. Ríos, and M. D. Stern. 1999. Amplitude distribution of calcium sparks in confocal images: theory and studies with an automatic detection method. *Biophys. J.* 76:606–617.

Colquhoun, D., and A. G. Hawkes. 1995. The principles of the stochastic interpretation of ion-channel mechanisms. *In* Single Channel Recording, Chapt. 18, 2nd Ed. B. Sakmann, and E. Neher, editors. Plenum Press, New York. 397–482.

Diaz, M. E., S. J. Cook, J. P. Chamunorwa, A. W. Trafford, M. K. Lancaster, S. C. O'Neill, and D. A. Eisner. 1996. Variability of spontaneous Ca^{2+} release between different rat ventricular myocytes is correlated with Na^+-Ca^{2+} exchange and $[Na^+]_i$. *Circ. Res.* 78:857–862.

Endo, M., M. Tanaka, and Y. Ogawa. 1970. Calcium-induced release of calcium from the sarcoplasmic reticulum of skinned skeletal muscle fibres. *Nature.* 228:34–36.

Fabiato, A. 1985. Time and calcium dependence of activation and inactivation of calcium-induced release of calcium from the sarcoplasmic reticulum of a skinned canine cardiac Purkinje cell. *J. Gen. Physiol.* 85:247–289.

Franzini-Armstrong, C., and F. Protasi. 1997. Ryanodine receptors of striated muscles: a complex channel capable of multiple interactions. *Physiol. Rev.* 77:699–729.

González, A., W. G. Kirsch, N. Shirokova, G. Pizarro, G. Brum, I. N. Pessah, M. D. Stern, H. Cheng, and E. Ríos. 2000a. Involvement of multiple intracellular release channels in calcium sparks of skeletal muscle. *Proc. Natl. Acad. Sci. U.S.A.* 97:4380–4385.

González, A., W. G. Kirsch, N. Shirokova, G. Pizarro, M. D. Stern, and E. Ríos. 2000b. The spark and its ember: separately gated local components of Ca^{2+} release in skeletal muscle. *J. Gen. Physiol.* 115:139–158.

Gration, K. A., J. J. Lambert, R. L. Ramsey, R. P. Rand, and P. N. Usherwood. 1982. Closure of membrane channels gated by glutamate receptors may be a two-step process. *Nature.* 295:599–603.

Haak, L. L., L. S. Song, T. F. Molinski, I. N. Pessah, H. Cheng, and J. T. Russell. 2001. Sparks and puffs in oligodendrocyte progenitors: cross talk between ryanodine receptors and inositol trisphosphate receptors. *J. Neurosci.* 21:3860–3870.

Hong, K., M. Nishiyama, J. Henley, M. Tessier-Lavigne, and M.-M. Poo. 2000. Calcium signalling in the guidance of nerve growth by netrin-1. *Nature.* 403:93–98.

Izu, L. T., J. R. Mauban, C. W. Balke, and W. G. Wier. 2001. Large currents generate cardiac Ca^{2+} sparks. *Biophys. J.* 80:88–102.

Izu, L. T., W. G. Wier, and C. W. Balke. 1998. Theoretical analysis of the Ca^{2+} spark amplitude distribution. *Biophys. J.* 75:1144–1162.

Klein, M. G., H. Cheng, L. F. Santana, Y. H. Jiang, W. J. Lederer, and M. F. Schneider. 1996. Two mechanisms of quantized calcium release in skeletal muscle. *Nature.* 379:455–458.

Klein, M. G., A. Lacampagne, and M. F. Schneider. 1999. A repetitive mode of activation of discrete Ca^{2+} release events (Ca^{2+} sparks) in frog skeletal muscle fibres. *J. Physiol.* 515:391–411.

Lee, H. B., L. Xu, and G. Meissner. 1994. Reconstitution of the skeletal muscle ryanodine receptor: Ca^{2+} release channel protein complex into proteoliposomes. *J. Biol. Chem.* 269:13305–13312.

Marks, A. R. 1997. Intracellular calcium-release channels: regulators of cell life and death. *Am. J. Physiol. Heart Circ. Physiol.* 272:H597–H605.

Marx, S. O., K. Ondrias, and A. R. Marks. 1998. Coupled gating between individual skeletal muscle Ca^{2+} release channels (ryanodine receptors). *Science.* 281:818–821.

Marx, S. O., S. Reiken, Y. Hisamatsu, T. Jayaraman, D. Burkhoff, N. Rosemblit, and A. R. Marks. 2000. PKA phosphorylation dissociates FKBP12.6 from the calcium release channel (ryanodine receptor): defective regulation in failing hearts. *Cell.* 101:365–376.

Meissner, G. 1994. Ryanodine receptor/Ca^{2+} release channels and their regulation by endogenous effectors. *Annu. Rev. Physiol.* 56:485–508.

Nelson, M. T., H. Cheng, M. Rubart, L. F. Santana, A. D. Bonev, H. J. Knot, and W. J. Lederer. 1995. Relaxation of arterial smooth muscle by calcium sparks. *Science.* 270:633–637.

Pape, P. C., D. S. Jong, and W. K. Chandler. 1995. Calcium release and its voltage dependence in frog cut muscle fibers equilibrated with 20 mM EGTA. *J. Gen. Physiol.* 106:259–336.

Parker, I., and W. G. Wier. 1997. Variability in frequency and characteristics of Ca^{2+} sparks at different release sites in rat ventricular myocytes. *J. Physiol.* 505:337–344.

Pratusevich, V. R., and C. W. Balke. 1996. Factors shaping the confocal image of the calcium spark in cardiac muscle cells. *Biophys. J.* 71:2942–2957.

Rengifo, J., W. G. Kirschl, E. Ríos, M. D. Stern, and A. González. 2001. Fast inactivation of Ca release in muscle: voltage-dependent aspects. *Biophys. J.* 80:1581*a*. (Abstr.).

Richard, E. A., and C. Miller. 1990. Steady-state coupling of ion-channel conformations to a transmembrane ion gradient. *Science.* 247:1208–1210.

Ríos, E., and G. Pizarro. 1991. Voltage sensor of excitation-contraction coupling in skeletal muscle. *Physiol. Rev.* 71:849–908.

Ríos, E., N. Shirokova, W. G. Kirsch, G. Pizarro, M. D. Stern, H. Cheng, and A. González. 2001. A preferred amplitude of calcium sparks in skeletal muscle. *Biophys. J.* 80:169–183.

Schneggenburger, R., and P. Ascher. 1997. Coupling of permeation and gating in an NMDA-channel pore mutant. *Neuron.* 18:167–177.

Shirokova, N., A. González, W. G. Kirsch, E. Ríos, G. Pizarro, M. D. Stern, and H. Cheng. 1999. Calcium sparks: release packets of uncertain origin and fundamental role. *J. Gen. Physiol.* 113:377–384.

Smith, G. D., J. E. Keizer, M. D. Stern, W. J. Lederer, and H. Cheng. 1998. A simple numerical model of calcium spark formation and detection in cardiac myocytes. *Biophys. J.* 75:15–32.

Soeller, C., and M. B. Cannell. 1997. Numerical simulation of local calcium movements during L-type calcium channel gating in the cardiac diad. *Biophys. J.* 73:97–111.

Song, L. S., J. S. Sham, M. D. Stern, E. G. Lakatta, and H. Cheng. 1998. Direct measurement of SR release flux by tracking "Ca^{2+} spikes" in rat cardiac myocytes. *J. Physiol.* 512:677–691.

Song, L. S., M. D. Stern, E. G. Lakatta, and H. Cheng. 1997. Partial depletion of sarcoplasmic reticulum calcium does not prevent calcium sparks in rat ventricular myocytes. *J. Physiol.* 505:665–675.

Stern, M. D., L. S. Song, H. Cheng, J. S. Sham, H. T. Yang, K. R. Boheler, and E. Rios. 1999. Local control models of cardiac excitation-contraction coupling: a possible role for allosteric interactions between ryanodine receptors. *J. Gen. Physiol.* 113:469–489.

Tinker, A., A. R. Lindsay, and A. J. Williams. 1992. A model for ionic conduction in the ryanodine receptor channel of sheep cardiac muscle sarcoplasmic reticulum. *J. Gen. Physiol.* 100:495–517.

Tripathy, A., and G. Meissner. 1996. Sarcoplasmic reticulum lumenal Ca^{2+} has access to cytosolic activation and inactivation sites of skeletal muscle Ca^{2+} release channel. *Biophys. J.* 70:2600–2615.

Tsugorka, A., E. Ríos, and L. A. Blatter. 1995. Imaging elementary events of calcium release in skeletal muscle cells. *Science.* 269:1723–1726.

Wang, S. Q., L. S. Song, E. G. Lakatta, and H. Cheng. 2001. Ca^{2+} signalling between single L-type Ca^{2+} channels and ryanodine receptors in heart cells. *Nature.* 410:592–596.

Xu, L., and G. Meissner. 1998. Regulation of cardiac muscle Ca^{2+} release channel by sarcoplasmic reticulum lumenal Ca^{2+}. *Biophys. J.* 75:2302–2312.

Zahradnikova, A., and I. Zahradnik. 1996. A minimal gating model for the cardiac calcium release channel. *Biophys. J.* 71:2996–3012.

Zahradnikova, A., I. Zahradnik, I. Gyorke, and S. Gyorke. 1999. Rapid activation of the cardiac ryanodine receptor by submillisecond calcium. *J. Gen. Physiol.* 114:787–798.

Zhou, Y. Y., S. Q. Wang, W. Z. Zhu, A. Chruscinski, B. K. Kobilka, Z. B. Ziman, S. Wang, E. G. Lakatta, H. Cheng, and R. P. Xiao. 2000. Culture and adenoviral infection of adult mouse cardiac myocytes: methods for cellular genetic physiology. *Am. J. Physiol. Heart Circ. Physiol.* 279:H429–H436.